Journal of Electroanalytical Chemistry 736 (2015) 16–21

Contents lists available at ScienceDirect

Journal of Electroanalytical Chemistry

journal homepage: www.elsevier.com/locate/jelechem

Coating of spinel $LiNi_{0.5}Mn_{1.5}O_4$ cathodes with SnO_2 by an electron cyclotron resonance metal–organic chemical vapor deposition method for high-voltage applications in lithium ion batteries

Yongho Lee [a,b], Tae Yong Kim [a,c], Dong-Won Kim [b], Joong Kee Lee [a,c], Wonchang Choi [a,c,*]

[a] Center for Energy Convergence, Korea Institute of Science and Technology, Hwarangno 14-gil 5, Seongbuk-gu, Seoul 136-791, Republic of Korea
[b] Department of Chemical Engineering, Hanyang University, 17 Haengdang-dong, Seongdong-gu, Seoul 133-791, Republic of Korea
[c] Department of Energy and Environmental Engineering, Korea University of Science and Technology (UST), 176 Gajung-dong, 217 Gajungro, Daejeon 305-350, Republic of Korea

ARTICLE INFO

Article history:
Received 18 August 2014
Received in revised form 16 October 2014
Accepted 19 October 2014
Available online 28 October 2014

Keywords:
Lithium ion battery
Lithium nickel manganese oxide
Surface modification
Tin oxide
Chemical vapor deposition

ABSTRACT

Tin oxide coating by employing electron cyclotron resonance metal–organic chemical vapor deposition was performed on 5 V-class spinel $LiNi_{0.5}Mn_{1.5}O_4$ cathode electrodes prepared by a conventional tape-casting method. The pristine and SnO_2-deposited $LiNi_{0.5}Mn_{1.5}O_4$ electrodes were characterized by X-ray diffraction, field-emission electron probe microanalyzer, field-emission scanning electron microscopy, Auger electron spectroscopy, charge–discharge measurements, and electrochemical impedance spectroscopy were evaluated in lithium cells using the fabricated electrodes. The SnO_2-deposited $LiNi_{0.5}Mn_{1.5}O_4$ electrodes exhibited better rate capability at room temperature and superior electrochemical performance during the storage test evaluated at 60 °C in a fully charged state than the pristine $LiNi_{0.5}Mn_{1.5}O_4$ electrode. Also, surface modification of the $LiNi_{0.5}Mn_{1.5}O_4$ electrode was found by impedance analyses to be effective for suppressing the increase of the charge transfer resistance during the storage test at elevated temperatures.

1. Introduction

Rechargeable lithium ion batteries (LIBs) are considered the most promising energy storage technology for portable electronics, hybrid electric vehicles (HEV), and electric vehicles (EV) because of their high power and energy density. A good example of an LIB is $LiCoO_2$ (a lithium transition metal oxide) and graphite (carbon) electrodes. To preserve the good reversibility of lithium ion insertion/deinsertion, the structure of the cathode and the anode active materials should be stable during extensive cycling. The ability of $LiCoO_2$ and carbon to accommodate lithium ions without irreversible structural changes makes them ideal electrode materials. However, $LiCoO_2$ cathodes might be difficult to apply for large storage batteries for EVs and HEVs due to their high cost and toxicity. For these reasons, $LiCoO_2$ cathode materials have been replaced by various lithium transition metal oxides and phosphates [1–4]. $LiNi_{0.5}Mn_{1.5}O_4$ with a spinel structure is one of the most promising cathode materials for lithium secondary batteries due to good cycling properties, high stability, and outstanding power capability, as well as their low cost, the abundance of resources, and their nontoxicity. However, this material experiences severe degradation, especially in a highly oxidized state and at elevated temperatures mostly due to side reactions such as electrolyte decomposition, the structural instability of the cathode materials, and transition metal ion dissolution, as addressed in previous studies [5–10]. To resolve these problems, extensive research has been conducted and can be categorized as (i) substitution of a small portion of cations and anions in $LiNi_{0.5}Mn_{1.5}O_4$ and (ii) surface modification of the active material by using various materials to suppress the formation of HF and side reactions between the cathode and electrolyte [11–25]. Among these materials for surface modification [11–25], SnO_2 is attractive due to the various properties and applications such as gas sensor, solar cell, and anode materials for batteries [26,27]. Moreover, Cho et al. [24] and Wang et al. [25] reported the enhancement in electrochemical performances by SnO_2 coating to obtain the structural stability on the surface of $LiCoO_2$ or prevent the Mn dissolution of $LiMn_2O_4$ cathodes. To improve the electrochemical performance of a high-voltage spinel $LiNi_{0.5}Mn_{1.5}O_4$ cathode, we introduced a SnO_2 coating on a conventionally slurry-cast electrode, which consisted of $LiNi_{0.5}Mn_{1.5}O_4$ powder, a polymeric binder, and conducting carbon on aluminum

* Corresponding author at: Center for Energy Convergence, Korea Institute of Science and Technology, Hwarangno 14-gil 5, Seongbuk-gu, Seoul 136-791, Republic of Korea. Tel.: +82 2 958 5253; fax: +82 2 958 5229.
E-mail address: wonchangchoi@kist.re.kr (W. Choi).

http://dx.doi.org/10.1016/j.jelechem.2014.10.022
1572-6657/

foil, by employing an electron cyclotron resonance metal–organic chemical vapor deposition (ECR-MOCVD) technique near room temperature. The ECR-MOCVD method makes it possible to modify tape-cast electrodes directly because it can be performed at room temperature, thus preventing any detrimental impact on the polymeric binder and conducting carbon of the slurry-cast electrode.

2. Experimental

$LiNi_{0.5}Mn_{1.5}O_4$ particles with an average size of ca. 7–10 μm were obtained from the Tanaka Chemical Corporation (Japan). The slurry for the cathode electrodes was fabricated by blending the cathode powders, Denka Black®, and poly(vinylidene fluoride) (92:4:4 based on weight) in a solvent (*N*-methyl-w-pyrrolidone). Then, the slurry was uniformly cast onto aluminum foil (current collector), resulting in conventional tape-cast electrodes. The electrodes were dried under vacuum at 120 °C and then pressed under a constant load. Then, tin oxide was deposited on the tape-cast electrode by using the ECR-MOCVD system. The ECR-based deposition system consists of an ECR plasma zone and a deposition zone. To deposit the SnO_2 on the $LiNi_{0.5}Mn_{1.5}O_4$ electrodes in a vacuum state, the system was kept at a base pressure of 1.3×10^{-2} Pa with a turbomolecular pump with an additional rotary mechanical pump and a Roots blower pump. Tetra-methyl tin (TMT) was used as the precursor for the tin oxide coating. TMT was fed into the deposition chamber through the mass flow controller with Ar gas as the carrier gas; hydrogen gas was utilized to enhance and control the properties of the tin-based thin layer [28,29]. The samples were deposited under the following conditions: a working pressure of 1.33 Pa, a TMT flow rate of 4 sccm, an O_2 flow rate of 28.6 sccm, a hydrogen flow rate of 3.5 sccm, a deposition time of 3 min, a magnetic current of 165 A, and a microwave power of 800 W.

To confirm the SnO_2 coating and its morphology, the surfaces of the pristine and surface-modified $LiNi_{0.5}Mn_{1.5}O_4$ electrodes were examined by means of scanning electron microscopy (SEM, Hitachi S4500), electron probe X-ray microanalysis (EPMA, JEOL JXA-8900), Auger electron spectroscopy (AES, PHI-700 and LC-TOFMS LECO) and X-ray photoelectron spectroscopy (XPS, Ulvac-PHI(PHI 5000 VersaProbe). The penetration depth calibration of AES was calculated based on the sputter rate of 250 Å min^{-1} for SiO_2. The electrochemical evaluation of the cathode electrodes was performed using CR2032 coin cells at various C-rates between 3.5 and 4.9 V versus Li/Li^+ at room temperature and elevated temperature. The counter electrode was lithium metal, and 1.3 M $LiPF_6$ in 3:7 ethylene carbonate and ethyl methyl carbonate was used as the electrolyte. The separator was a polyethylene film (Tonen). The storage test was performed at 60 °C in the fully charged state, and the change in open-circuit voltage (OCV) of the electrodes during the storage test was evaluated daily at room temperature. AC impedance measurements were carried out with an AC amplitude of 5 mV in the frequency range of 10^6–10^{-3} Hz by a VSP-300, Biologic. The fittings of the data were carried out with ZView® software with a fit circle function.

3. Results and discussion

Fig. 1 is a schematic diagram of the process used to introduce the SnO_2 coating layer on the tape-cast cathode electrode by employing the ECR-MOCVD system. The ECR-based MOCVD process can be performed at room temperature without any harmful damage to electrode components such as active material, conducting agent, or polymeric binder, whereas most deposition techniques are performed at elevated temperatures. Using the current method, the tin oxide layer is directly applied onto the conventionally

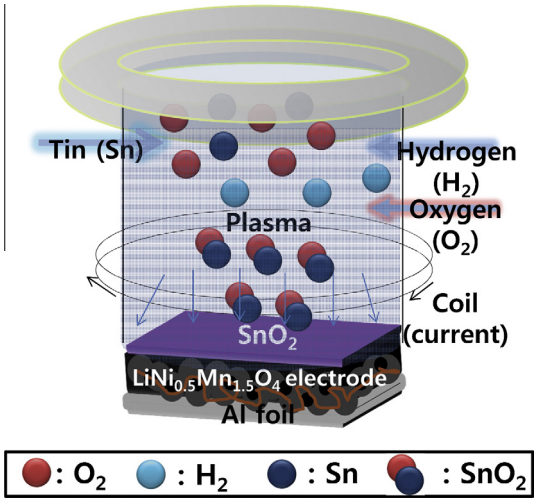

Fig. 1. Schematic diagram of SnO_2 deposition process on the 5 V Spinel $LiNi_{0.5}Mn_{1.5}O_4$ cathode electrodes by ECR-MOCVD.

tape-cast electrode. XPS analysis reveals that the chemical composition of coating layer obtained from ECR-MOCVD system is SnO_2, as shown in Fig. S1.

Fig. 2 reveals the SEM images of the cross-sectional view and the corresponding EPMA mapping for the pristine and SnO_2-deposited $LiNi_{0.5}Mn_{1.5}O_4$ electrodes [30]. Although the existence of the coating layer after the coating process cannot be seen clearly from the cross-sectional SEM images of the electrodes, the EPMA results for Sn in Fig. 2b exhibits the evident and uniform coating layer on the cathode. Also, both electrodes do not show any notable difference or degradation in the surface morphology, suggesting that the deposition process by ECR-MOCVD is appropriate for modifying the surface characteristics of cathode electrodes. In order to determine the accurate thickness of the SnO_2 layer deposited on the cathode electrodes, AES analysis was performed. Fig. 3a shows the average atomic concentrations of oxygen, tin, manganese, and nickel as a function of the depth from the surface of the SnO_2-coated electrode. Although the existence and diffusion of tin can be found at a depth of more than 200 nm, the atomic concentrations of both tin and oxygen decreased significantly at approximately 75 nm, implying the successful surface coating of a thin SnO_2 layer on the tape-cast cathode electrode by ECR-MOCVD. The relative concentration of tin as compared to that of manganese also certifies that a distinguishable layer less than 100 nm was formed, as depicted in Fig. 3b.

Fig. 4 compares the initial charge and discharge profiles at the first cycle for the pristine and SnO_2-coated $LiNi_{0.5}Mn_{1.5}O_4$ electrodes. The cells were cycled at a current density of 70 mA g^{-1} between 3.5 and 4.9 V, which corresponds to a 0.5 C-rate evaluation. Both electrodes exhibited a flat voltage plateau at 4.7 V, which resulted from the Ni^{2+}/Ni^{4+} redox reaction, and a small voltage region at 4.0 V, which corresponds to the Mn^{3+}/Mn^{4+} redox process. Also, the pristine and SnO_2-deposited $LiNi_{0.5}Mn_{1.5}O_4$ electrodes exhibited similar discharge capacity values of approximately 135 mA h g^{-1}, indicating that the incorporation of the SnO_2 layer did not involve additional redox reactions related to lithium insertion/deinsertion or side reactions.

The rate capability of the pristine and surface-modified electrodes was evaluated between 3.5 and 4.9 V at various C-rates from 0.2 (28 mA g^{-1}) to 20 (3200 mA g^{-1}) during the discharge process, as presented in Fig. 5. All the cells were charged at a fixed current density of 0.2 C-rate (28 mA g^{-1}) before each discharge test. Although the discharge capacities evaluated at low current densities such as 0.2, 0.5, and 1 C-rate reveal similar values for both

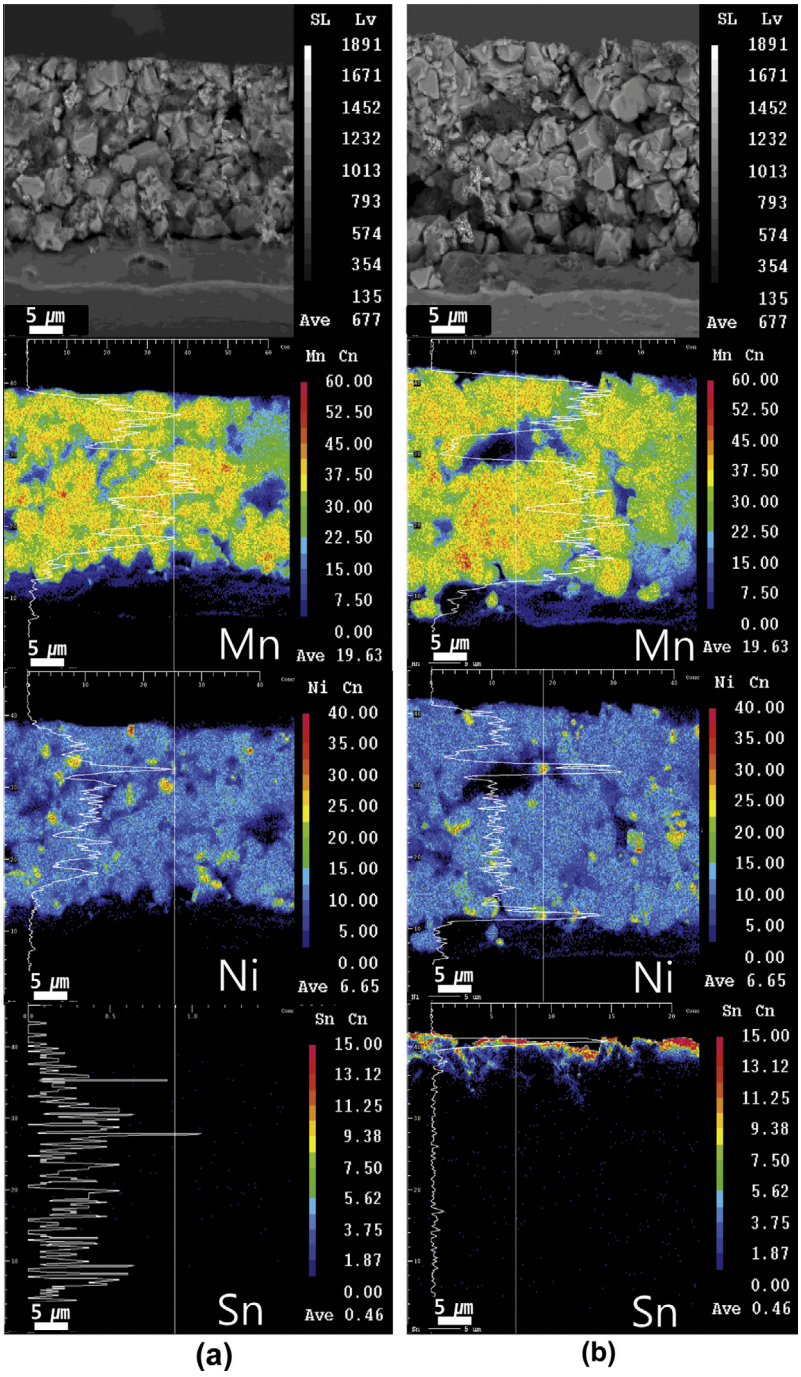

Fig. 2. SEM images of the cross-sectional view and the corresponding EPMA mapping of Mn, Ni, and Sn map for (a) pristine and (b) SnO_2-deposited $LiNi_{0.5}Mn_{1.5}O_4$ electrodes.

electrodes, the SnO_2-coated electrode exhibited enhanced rate capability, especially at high current densities above 2 C-rate. For example, at 20 C-rate, the SnO_2-deposited $LiNi_{0.5}Mn_{1.5}O_4$ electrode showed a capacity of 72.0 mA h g^{-1}, whereas the pristine $LiNi_{0.5}Mn_{1.5}O_4$ electrode delivered only 53.9 mA h g^{-1} in the cycled voltage range.

The discharge profiles in Fig. 5 were analyzed to elucidate the relation between the rate capability and polarization resistance (R_p) for the pristine and surface-modified electrodes and the results are shown in Fig. 6. Utilizing the domain ranging from 10 to 70% depth of discharge (DOD), in which the voltage presents a linear relationship with the current shown in Fig. 5, the plots of voltage against current for the pristine and surface-modified electrodes were obtained and are shown in Fig. 6a and b, respectively. Then, the R_p values for the pristine and SnO_2-coated electrodes were calculated based on the relation $R_p = V/I$ and the results are shown in Fig. 6c. Both electrodes exhibit a prominent increase of R_p with increasing DOD, indicating that the electrochemical insertion of lithium is influenced by the kinetic properties resulting from the accumulation of lithium during the discharge process. This result is also in agreement with other studies [19,31]. Interestingly, the surface-modified electrode exhibits suppressed R_p values in a given range of DOD as compared to the pristine cathode electrodes, suggesting that the surface coating by ECR-MOCVD enhances the chemical stability of the electrodes during the lithium insertion process [19].

Fig. 7a compares the cycling performance of the pristine and SnO_2-coated $LiNi_{0.5}Mn_{1.5}O_4$ electrodes for 100 cycles with a current

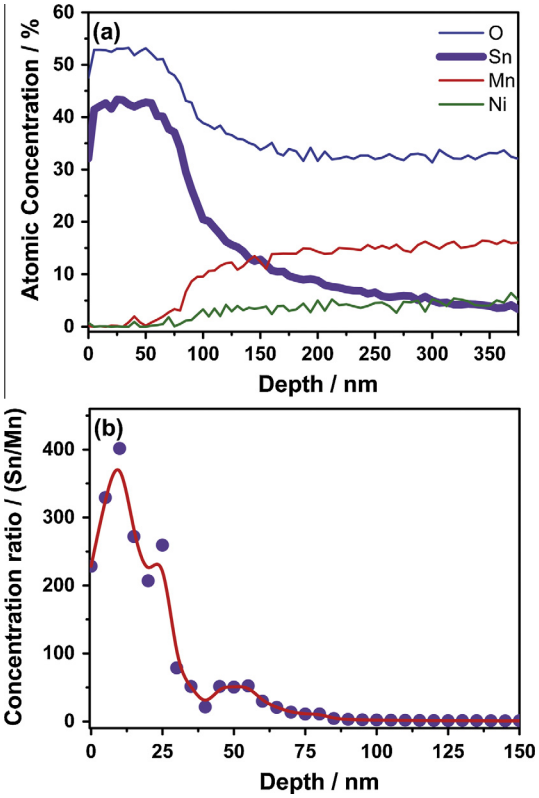

Fig. 3. Auger electron spectroscopy depth profiles of the SnO_2-deposited $LiNi_{0.5}Mn_{1.5}O_4$ electrode: (a) atomic concentrations of O, Sn, Mn, and Ni and (b) concentration ratio of Sn to Mn as a function of depth from surface.

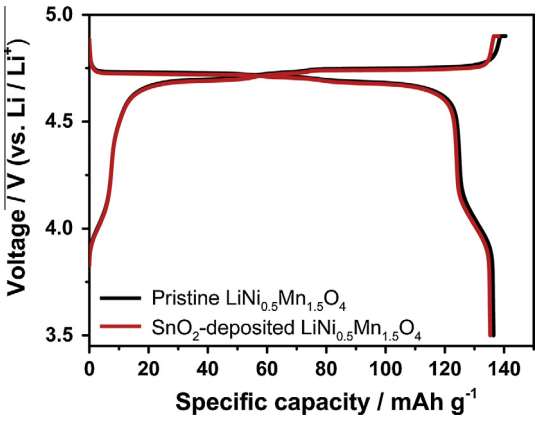

Fig. 4. The charge–discharge curves at the first cycle for the pristine and SnO_2-deposited $LiNi_{0.5}Mn_{1.5}O_4$ electrodes.

rate of 1 C at room temperature. Both electrodes show favorable performance for 100 cycles and similar differential capacity curves after 100 cycles, although the SnO_2-deposited $LiNi_{0.5}Mn_{1.5}O_4$ electrode exhibits a slightly better capacity retention of 95.21% than the pristine $LiNi_{0.5}Mn_{1.5}O_4$ electrode with a capacity retention of 86.14% after 100 cycles. However, a subsequent storage test at a fully charged state and 60 °C for 4 days reveals dramatic differences in the electrochemical performance of the pristine and surface-modified electrodes, as demonstrated in Fig. 7b and c. The surface-modified electrode maintained its open-circuit voltage (OCV) of approximately 4.7 V at a fully charged state and 60 °C for 4 days, whereas the pristine electrode exhibited an abrupt decrease in OCV between 3 and 4 days, which suggests a severe

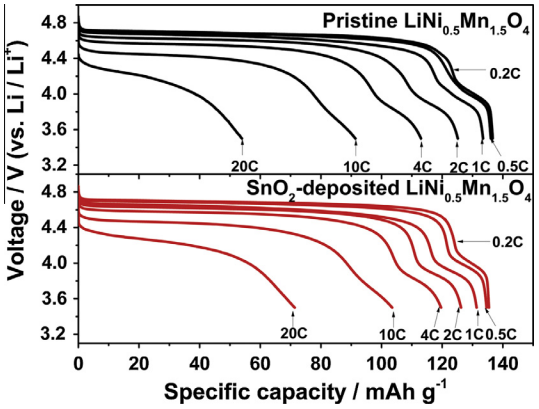

Fig. 5. Discharge profiles illustrating the rate capability of the pristine and SnO_2-deposited $LiNi_{0.5}Mn_{1.5}O_4$ electrodes.

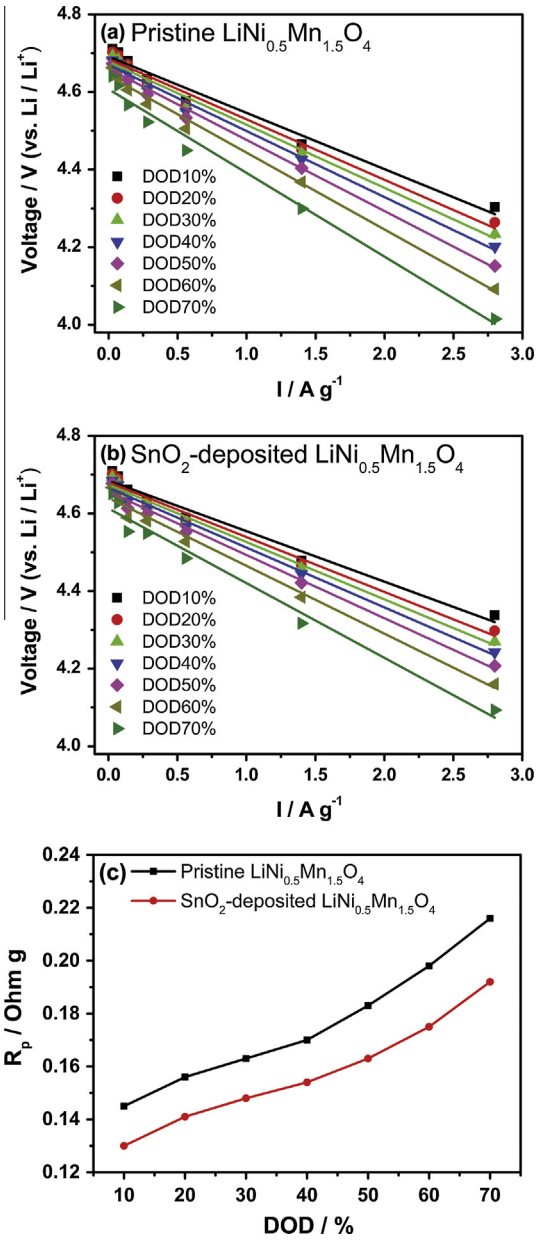

Fig. 6. Relationship between voltage and current density at different depths of discharge for the (a) pristine and (b) SnO_2-deposited $LiNi_{0.5}Mn_{1.5}O_4$ electrodes. (c) Variations of the polarization resistance with depth of discharge for the pristine and the SnO_2-deposited $LiNi_{0.5}Mn_{1.5}O_4$ electrodes.

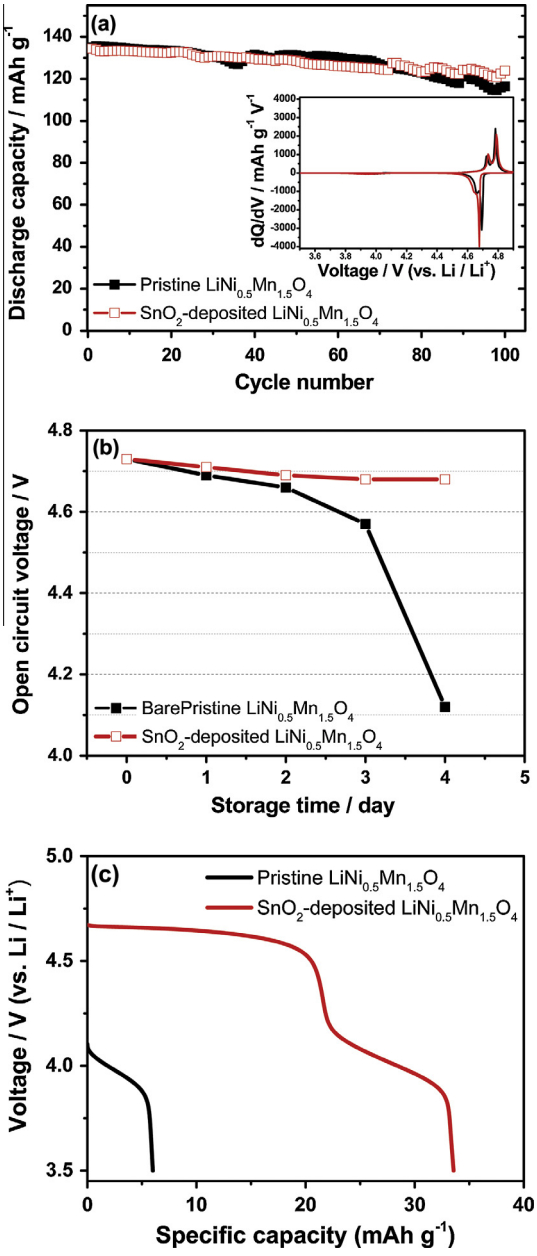

Fig. 7. Electrochemical performances of the pristine and SnO_2-deposited $LiNi_{0.5}Mn_{1.5}O_4$ electrodes. (a) Cycling performance evaluated for 100 cycles between 3.5 and 4.9 V at room temperature. The inset shows the corresponding capacity plots at the 100th cycle. (b) Evaluation of open-circuit voltage during the storage test for 4 days at 60 °C for the 100 cycle electrodes. (c) Discharge curves of capacity retention after the storage test for 4 days at 60 °C for the 100 cycle electrodes.

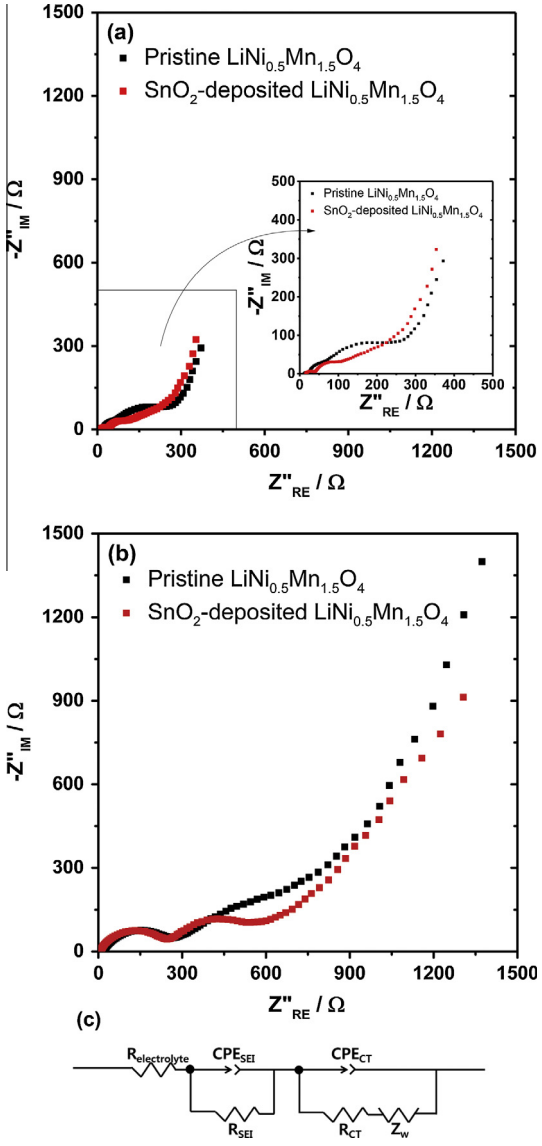

Fig. 8. EIS spectra of the pristine and SnO_2-deposited $LiNi_{0.5}Mn_{1.5}O_4$ electrodes after (a) 3 cycles at room temperature and (b) storage for 2 weeks at 60 °C. (c) Equivalent circuit for the pristine and SnO_2-deposited $LiNi_{0.5}Mn_{1.5}O_4$ electrodes.

self-discharge reaction, mostly due to the side reaction between the electrode and electrolyte. The discharge capacity evaluation after the storage test at 60 °C for 4 days, as presented in Fig. 7c, also certifies a suppressed self-discharge reaction with surface modification during the storage test at elevated temperatures, indicating the higher discharge capacity of the surface-modified electrode of approximately 35 mA h g^{-1} as compared to that of the pristine electrode of approximately 6 mA h g^{-1}.

As the self-discharge reaction resulting from the side reaction between electrode and electrolyte generally lead to the deterioration of electrodes, formation of unwanted SEI film, and subsequent degradation in electrochemical performances, AC impedance evaluation was performed before and after the storage test at 60 °C for 2 weeks to confirm the effect of surface-modification and the influence of high temperature environment and highly oxidized state for high-voltage spinel $LiNi_{0.5}Mn_{1.5}O_4$ cathodes. The Nyquist plots obtained are presented in Fig. 8. Also, the empirical impedance data were fitted by employing the equivalent circuit shown in Fig. 8c, and the corresponding calculated numerical values are presented in Table 1. In the equivalent circuit, $R_{electrolyte}$ is the electrolyte resistance, R_{SEI} (first semicircle at high frequency) refers to the diffusion resistance of Li^+ through the solid

Table 1
Fitting results of Nyquist plots using the equivalent circuit of the pristine and SnO_2-deposited $LiNi_{0.5}Mn_{1.5}O_4$ electrode.

	After 3 cycles			After storage for 2 weeks at 60 °C		
	$R_{electrolyte}$ (Ω)	R_{SEI} (Ω)	R_{CT} (Ω)	$R_{electrolyte}$ (Ω)	R_{SEI} (Ω)	R_{CT} (Ω)
Pristine LNMO	11.4	46.6	214.5	18.5	232.7	716.5
SnO_2-deposited LNMO	14.6	60.9	254.9	7.3	240	301.9

electrolyte interface (SEI) e layers, including the SEI and deposited layers, CPE_{SEI} corresponds to the non-ideal capacitance of the surface layer, R_{CT} (second semicircle at medium frequency) is the charge transfer resistance, CPE_{CT} represents the non-ideal capacitance of the double layer, and Z_w (at low frequency) is related to the solid-state diffusion of Li^+ corresponding to Warburg impedance [18,19,21]. As seen in Table 1, differences in the $R_{electrolyte}$ values obtained before and after the storage test are negligible, and the R_{SEI} values after the storage test exhibited a similar increase for both the pristine and the SnO_2-deposited electrodes. In contrast, the pristine electrodes showed a significant increase in the R_{CT} value after the storage test as compared to the SnO_2-deposited electrodes. As the formation and role of SEI film on cathode materials is generally known to be small compared to the anode materials, the prominent increase in R_{CT} suggest the degradation on the surface of active material resulting from the side reaction between electrode and electrolyte. This result implies that the surface modification of the electrodes is also effective for suppressing the polarization resistance increase, especially the charge transfer resistance under highly oxidized conditions and at elevated temperature.

4. Conclusions

A tape-cast spinel $LiNi_{0.5}Mn_{1.5}O_4$ electrode was modified with tin oxide by employing the ECR-MOCVD technique, and the presence of effective surface coating on a conventionally prepared cathode was confirmed by FE-SEM, EPMA, and AES analyses. Surface modification of cathode electrodes with tin oxide led to the electrochemical enhancement of the rate characteristics at room temperature. The storage test evaluated at 60 °C in a fully charged state revealed that the SnO_2-coated electrode exhibited better retention of charge capacity, whereas the pristine electrode exhibited a severe self-discharge reaction, possibly due to a side reaction between the cathode and electrolyte. Further investigation using electrochemical impedance spectroscopy before and after the storage test at elevated temperature indicated that surface coating onto the tape-cast electrode inhibits the increase in the charge transfer resistance of high-voltage spinel cathode materials.

Conflict of interest

There is no conflict of interest.

Acknowledgements

This work was supported by the National Research Foundation of Korea Grant funded by the Korean Government (MEST) (NRF-2010-C1AAA001-2010-0028958), and the KIST Institutional Program (Project No. 2E24554).

Appendix A. Supplementary material

Supplementary data associated with this article can be found, in the online version, at http://dx.doi.org/10.1016/j.jelechem.2014.10.022.

References

[1] M.M. Thackeray, P.J. Johnson, L.A. de Picciotto, P.G. Bruce, J.B. Goodenough, Mater. Res. Bull. 19 (1984) 179–187.
[2] M.S. Whittingham, Chem. Rev. 104 (2004) 4271–4301.
[3] K.M. Shaju, P.G. Bruce, Adv. Mater. 18 (2006) 2330–2334.
[4] A.K. Padhi, K.S. Najundaswamy, J.B. Goodenough, J. Electrochem. Soc. 144 (1997) 1188–1194.
[5] H. Duncan, D. Duguay, Y. Abu-Lebdeh, I.J. Davidson, J. Electrochem. Soc. 158 (2011) A537–A545.
[6] D. Aurbach, B. Markovsky, Y. Talyossef, G. Salitra, H.J. Kim, S. Choi, J. Power Sources 162 (2006) 780–789.
[7] Y. Talyosef, B. Markovsky, R. Lavi, G. Salitra, D. Aurbach, D. Kovacheva, M. Gorova, E. Zhecheva, R. Stoyanova, J. Electrochem. Soc. 154 (2007) A682–A691.
[8] U. Lafont, C. Locati, W.J.H. Borghols, A. Lasinska, J. Dygas, A.V. Chadwick, E.M. Kelder, J. Power Sources 189 (2009) 179–184.
[9] R. Santhanam, B. Rambabu, J. Power Sources 195 (2010) 5442–5451.
[10] B. Markovsky, Y. Talyossef, G. Salitra, D. Aurbach, H.J. Kim, S. Choi, Electro. Comm. 6 (2004) 821–826.
[11] J.M. Tarascon, W. McKinnon, F. Coowar, T. Bowmer, G. Amatucci, D. Guyomard, J. Electrochem. Soc. 141 (1994) 1421–1431.
[12] A.D. Robertson, S.H. Lu, W.F. Averill, W.F. Howard, J. Electrochem. Soc. 144 (1997) 3500–3505.
[13] J.H. Lee, J.K. Hong, D.H. Jang, Y.K. Sun, S.M. Oh, J. Power Sources 89 (2000) 7–14.
[14] Y.K. Sun, Y.S. Jeon, H.J. Lee, Electrochem. Solid State Lett. 3 (2000) 7–9.
[15] Y. Fan, J. Wang, Z. Tang, W. He, J. Zhang, Electrochim. Acta 52 (2007) 3870–3875.
[16] J.Y. Shi, C.W. Yi, K. Kim, J. Power Sources 195 (2010) 6860–6866.
[17] J.C. Arrebola, A. Caballero, L. Hernan, J. Morales, J. Power Sources 195 (2010) 4278–4284.
[18] T. Noguchi, I. Yamazaki, T. Numata, M. Shirakata, J. Power Sources 174 (2007) 359–365.
[19] J. Liu, A. Manthiram, Chem. Mater. 21 (2009) 1695–1707.
[20] H.B. Kang, S.T. Myung, K. Amine, S.M. Lee, Y.K. Sun, J. Power Sources 195 (2010) 2023–2028.
[21] H.M. Wu, I. Belharouak, A. Abouimrane, Y.K. Sun, K. Amine, J. Power Sources 195 (2010) 2909–2913.
[22] J. Liu, A. Manthiram, J. Electrochem. Soc. 156 (2009) A833–A838.
[23] J. Liu, A. Manthiram, J. Electrochem. Soc. 156 (2009) A66–A72.
[24] J. Cho, C.S. Kim, S.I. Yoo, Electrochem. Solid State Lett. 3 (2000) 362–365.
[25] L. Wang, J. Zhao, S. Guo, X. He, C. Jiang, C. Wan, Int. J. Electrochem. Sci. 5 (2010) 1113–1126.
[26] Z. Wang, G. Chen, D. Xia, J. Power Sources 184 (2008) 432–436.
[27] D. Chandra, N. Mukherjee, A. Mondal, A. Bhaumik, J. Phys. Chem. C 112 (2008) 8668–8674.
[28] B.J. Jeon, J.K. Lee, J. Mater. Sci. 41 (2006) 6274–6279.
[29] J.H. Park, D. Byun, J.K. Lee, Surf. Coat. Technol. 205 (2010) S144–S145.
[30] K. Nagata, T. Nanno, J. Power Sources 174 (2007) 832–837.
[31] C. Delacourt, L. Laffont, R. Bouchet, C. Wurm, J.B. Leriche, M. Morcrette, J.M. Tarascon, C. Masquelier, J. Electrochem. Soc. 152 (2005) A913–A921.